THE JOURNAL OF BIOLOGICAL CHEMISTRY
Vol. 279, No. 23, Issue of June 4, pp. 24485–24492, 2004
Printed in U.S.A.

Biochemical Differences in the $\alpha\beta$ T Cell Receptor·CD3 Surface Complex between CD8$^+$ and CD4$^+$ Human Mature T Lymphocytes*

Received for publication, October 20, 2003, and in revised form, February 27, 2004
Published, JBC Papers in Press, April 1, 2004, DOI 10.1074/jbc.M311455200

David A. Zapata‡§, Wolfgang W. A. Schamel¶, Pilar S. Torres‡§, Balbino Alarcón¶, Nineth E. Rossi‡‖, María N. Navarro¶, María L. Toribio¶, and José R. Regueiro‡**

From the ‡Inmunología, Facultad de Medicina, Universidad Complutense, 28040 Madrid, Spain and the ¶Centro de Biología Molecular Severo Ochoa, Consejo Superior de Investigaciones Científicas, Universidad Autónoma, Cantoblanco, 28049 Madrid, Spain

We have reported the existence of biochemical and conformational differences in the $\alpha\beta$ T cell receptor (TCR) complex between CD4$^+$ and CD8$^+$ CD3γ-deficient (γ^-) mature T cells. In the present study, we have furthered our understanding and extended the observations to primary T lymphocytes from normal (γ^+) individuals. Surface TCR·CD3 components from CD4$^+$ γ^- T cells, other than CD3γ, were detectable and similar in size to CD4$^+$ γ^+ controls. Their native TCR·CD3 complex was also similar to CD4$^+$ γ^+ controls, except for an $\alpha\beta(\delta\epsilon)_2\zeta_2$ instead of an $\alpha\beta\gamma\epsilon\delta\epsilon\zeta_2$ stoichiometry. In contrast, the surface TCRα, TCRβ, and CD3δ chains of CD8$^+$ γ^- T cells did not possess their usual sizes. Using confocal immunofluorescence, TCRα was hardly detectable in CD8$^+$ γ^- T cells. Blue native gels (BN-PAGE) demonstrated the existence of a heterogeneous population of TCR·CD3 in these cells. Using primary peripheral blood T lymphocytes from normal (γ^+) donors, we performed a broad epitopic scan. In contrast to all other TCR·CD3-specific monoclonal antibodies, RW2-8C8 stained CD8$^+$ better than it did CD4$^+$ T cells, and the difference was dependent on glycosylation of the TCR·CD3 complex but independent of T cell activation or differentiation. RW2-8C8 staining of CD8$^+$ T cells was shown to be more dependent on lipid raft integrity than that of CD4$^+$ T cells. Finally, immunoprecipitation studies on purified primary CD4$^+$ and CD8$^+$ T cells revealed the existence of TCR glycosylation differences between the two. Collectively, these results are consistent with the existence of conformational or topological lineage-specific differences in the TCR·CD3 from CD4$^+$ and CD8$^+$ wild type T cells. The differences may be relevant for *cis* interactions during antigen recognition and signal transduction.

$\alpha\beta$ T lymphocytes recognize peptide-major histocompatibility complex ligands by means of a multimeric protein complex termed the $\alpha\beta$ T cell receptor (TCR)[1] CD3 complex (TCR·CD3). This structure is composed of a variable $\alpha\beta$ TCR dimer that binds antigens and three invariant dimers (CD3$\gamma\epsilon$, $\delta\epsilon$, and $\zeta\zeta$) that are in charge of TCR·CD3 complex transport, stabilization, and signal transduction (1). The minimum stoichiometry, therefore, is believed to be $\alpha\beta\gamma\epsilon\delta\epsilon\zeta_2$.

Mature CD4$^+$ and CD8$^+$ $\alpha\beta$ T cells differ sharply in their major histocompatibility complex ligands, but their TCR·CD3 complex is believed to be qualitatively identical. The reduced $\alpha\beta$ TCR·CD3 staining levels observed in CD8$^+$ T cells, relative to CD4$^+$ T cells, were therefore reported as quantitative under this assumption (2). Unexpectedly, peripheral blood $\alpha\beta$ TCR·CD3 expression was shown to be more impaired in CD8$^+$ than in CD4$^+$ cells when CD3γ (3, 4) or CD3δ (5) was absent. These observations were followed by the description of conformational and biochemical differences in the TCR·CD3 complex between CD8$^+$ and CD4$^+$ CD3γ deficient (γ^-) T lymphocytes (6). Biosynthetic studies showed that CD8$^+$ but not CD4$^+$ γ^- T cells lacked normal TCRα. Instead, the CD4$^+$ γ^- T cells contained a small $\alpha\beta$ heterodimer composed of abnormally glycosylated TCRβ and an abnormally small CD3-associated chain that was not recognized by TCRα-specific antibodies.

In the present study, we have extended these biochemical studies to the cell surface and provide further evidence for the existence of qualitative differences in the $\alpha\beta$ TCR·CD3 complex between CD8$^+$ and CD4$^+$ T lymphocytes, particularly when CD3γ is lacking, but also in normal T cells.

EXPERIMENTAL PROCEDURES

Cells—Herpesvirus saimiri-transformed T cell lines were derived with informed consent from the peripheral blood lymphocytes (PBLs) of a healthy congenital CD3γ-deficient (γ^-) individual or the PBLs of normal donors (γ^+) as described previously (7, 8). The T cell lines used in the experiments (DSF4, CD4$^+$ γ^-; CTRCD4, CD4$^+$ γ^+; DSF8, CD8$^+$ γ^-; and CTO, CD8$^+$ γ^+) had been cultured for 6–7 years when the experiments were performed. Cells had always been grown in parallel in 1:1 RPMI 1640 and 25 mM Hepes/Panserin medium (from Invitrogen and Pan Biotech, Aidenbach, Germany, respectively) supplemented with 40 IU/ml human rIL-2 (Frederick Cancer Research and Development Center, NCI, National Institutes of Health, Frederick, MD), 10% FCS (Flow Laboratories), and 1% glutamine (BioWhitaker, Berkshire, UK). The medium was replaced every 3–4 days. The pre-TCR-expressing cell line SupT1 was grown in RPMI 1640 and 25 mM Hepes supplemented with 10% FCS and 1% glutamine.

Human PBLs were obtained with informed consent from normal donors. Purified CD4$^+$ and CD8$^+$ T cells were isolated immunomagnetically using standard procedures according to manufacturer's instructions (Miltenyi Biotec, Bergisch Gladbach, Germany). Purities >90% were the rule. Human postnatal thymocytes were isolated from thymus fragments removed during corrective cardiac surgery of patients aged 1 month to 4 years with informed parental consent.

TCR Labeling and Immunoprecipitation—Surface labeling (^{125}I and

---

* This work was supported by grants from the Ministerio de Ciencia y Tecnología (BMC2002-3247) and the Comunidad Autónoma de Madrid (21/01) (to J. R. R.). The costs of publication of this article were defrayed in part by the payment of page charges. This article must therefore be hereby marked "*advertisement*" in accordance with 18 U.S.C. Section 1734 solely to indicate this fact.

§ Supported by Comunidad Autónoma de Madrid.

‖ Supported by the Universidad de Los Andes (Venezuela).

** To whom correspondence should be addressed. Tel.: 34-91-394-1642; Fax: 34-91-394-1641; E-mail: regueiro@med.ucm.es.

[1] The abbreviations used are: TCR, T cell receptor; BN, blue native; FCS, fetal calf serum; mAb, monoclonal antibody; MβCD, methyl-β-cyclodextrin; MFI, mean fluorescence intensity; NANAse, *N*-acetylneuraminidase; PBL, peripheral blood lymphocyte.

biotin) and precipitation experiments were performed as described in Refs. 6 and 7. Cells were ^{125}I-labeled using the lactoperoxidase method. Samples were lysed in Nonidet P-40 (Sigma)-containing lysis buffer (1% Nonidet P-40, 150 mM NaCl, 20 mM Tris-HCl, pH 8, 10 mM iodoacetamide, and 1 mM phenylmethylsulfonyl fluoride) or in digitonin (or Brij96)-containing lysis buffer (1% digitonin (or Brij96), 50 mM Tris-HCl, 150 mM NaCl, 1 mM $MgCl_2$, 0.1 mM EDTA, 1 mM phenylmethylsulfonyl fluoride, and 8 mM iodoacetamide). Supernatants, hereafter referred to as lysates, were collected and transferred to new tubes. The lysates were precleared twice with Sepharose beads (Amersham Biosciences) containing 1% Nonidet P-40 or 1% digitonin (or Brij96, depending on the detergent used for the lysis), followed by a 2-min centrifugation at 12,000 × *g* in an Eppendorf centrifuge at 4 °C. The precleared supernatants were subsequently immunoprecipitated for 1 h and 30 min at 4 °C with 5–10 μl of an TCRα- or TCRβ-specific mAb (αF1 and βF1, respectively, from Endogen, Cambridge, MA) or 0.5 ml of the CD3-specific mAb OKT3 (CD3εγ/εδ-specific, generously donated by Dr. Bent Rubin, Centre Hospitaliare Universitaire de Purpan, Toulouse, France) coupled to protein G-Sepharose beads (Amersham Biosciences). For control immunoprecipitations, 5–10 μl of W6/32 mAb supernatant (a gift from Dr. E. Martínez-Naves, Inmunología, Universidad Complutense) coupled to protein-G-Sepharose beads were used. The beads were afterward washed 5 times in lysis buffer.

Endo-β-*N*-acetylglucosaminidase H and *N*-glycosidase F (Roche Applied Science) treatments were done as described (6, 7). Finally, samples were resuspended in Laemmli sample buffer and boiled for 5 min before a short spin at 12,000 × *g*. SDS-PAGE was performed on 10% polyacrylamide gels and analyzed by autoradiography.

Confocal Microscopy—5 × 10^6 cells were washed twice in phosphate-buffered saline/1% bovine serum albumin and adjusted to a final concentration of 2.5 × 10^5/ml in the same solution. 2.5 × 10^4 cells were dropped on non-treated glass slides by cytocentrifugation at 400 rpm for 3–4 min in a Cytospin 3 cytocentrifuge (Shandon, Pittsburgh, PA). Samples were air-dried and then fixed in acetone at room temperature for 5 min. Slides were again air-dried and subsequently stained with the corresponding mAb. Briefly, 100 μl of either TCRα- or TCRβ-specific mAb (1:5 dilution) were dispensed onto the fixed cells, and the slides were incubated at room temperature in a wet box for 40 min. Samples were washed twice in phosphate-buffered saline, dried carefully, and stained with a mouse IgG-specific Cy5-conjugated secondary mAb (100 μl, 1:200 dilution) for another 40 min in a wet box. After two more washes with phosphate-buffered saline, samples were dried and stained (40 min, wet box) with either CD4- or CD8α-specific fluorescein isothiocyanate-conjugated mAb from Pharmingen (100 μl, 1:2 dilution). After two final washes, a drop of 1,4-diazabicyclo[2.2.2]octane (DABCO) mounting medium was added to the slides, and cells were analyzed under a Bio-Rad MRC-1024 confocal microscope.

Flow Cytometry—TCR·CD3-associated epitopes were analyzed in thymocytes, PBLs, or *H. saimiri*-transformed T cells by three-color flow cytometry as described elsewhere (30 min, 4 °C; Ref. 8). PBLs were studied either before or 12 h after phytohemagglutinin stimulation (Sigma; 5 μg/ml; Ref. 9). Briefly, 5 × 10^5 cells were stained with CD3- or TCR-specific mAb, washed twice in phosphate-buffered saline/1% FCS, and stained with a fluorescein isothiocyanate-conjugated panTγδ mAb and a PC5-conjugated CD4- or CD8-specific mAb so that lineage-dependent comparisons could be established within γδ$^-$ CD4$^+$- or γδ$^-$ CD8$^+$-gated PBL subsets. Other PBL subsets were defined and gated using the appropriate mAb (CD45RA, CD45RO, or CD69). Intrathymic, mature, single positive subsets were gated as CD4$^+$CD8$^-$CD3$^+$ or CD4$^+$CD8$^-$CD1a$^-$ and CD4$^-$CD8$^+$γδ$^-$ or CD4$^-$CD8$^+$CD1a$^-$γδ$^-$, respectively, or analyzed after magnetic sorting using CD1a-coated microbeads (Miltenyi Biotec). For comparative stainings, the mean fluorescence intensity (MFI) was used.

The mAbs used in the study were UCHT1 (CD3εγ/εδ), CD4, CD8, and CD45RO from Immunotech (Marseille, France); X35 (CD3ε) from D. Bourel (Centre Régional de Transfusion Sanguine, Rennes, France); 2Ad2 (CD3ε) and RW2-8C8 (CD3ε) from E. L. Reinherz (Dana-Farber Cancer Institute, Boston, MA); SPV.T3b (CD3ε) from J. E. de Vries (The Netherlands Cancer Institute, Amsterdam, The Netherlands); F101.01 (CD3) hybridoma supernatant from Dr. Bent Rubin; Cris7 (CD3ε) from R. Vilella (Hospital Clínico, Barcelona, Spain); WT31 (CD3ε), Leu4 (CD3εγ/εδ), SP34 (CD3ε), CD8, CD69, CD45RA, and CD43 from BD Biosciences; BMA031 (TCRαβ) from Caltag or Beckman Coulter; CD4 and CD1a from Beckman Coulter; TS2/16 and Lia 3/2 (CD18) from C. Cabañas (Instituto de Farmacología y Toxicología, CSIC-UCM, Facultad de Medicina, Universidad Complutense, Madrid, Spain); TCRδ1 (TCRγδ) from T Cell Diagnostics (Boston, MA) or Caltag. For purified mAb, phycoerythrin-conjugated goat anti-mouse IgG (H+L) or IgM (μ) secondary antibodies from Caltag, Southern Biotechnology Associates, or Immunotech were used.

To selectively disrupt lipid rafts, cholesterol was removed using methyl-β-cyclodextrin (MβCD; Sigma) as described (10). MβCD was dissolved in water (0.5 M) and diluted in Dulbecco's modified Eagle's medium containing 50 mM Hepes buffer. Briefly, 2 × 10^6 purified PBLs were washed in RPMI 1640 and 1% FCS, treated with 10 mM MβCD for 30 min at 37 °C, and then washed extensively in ice-cold RPMI 1640 and 1% FCS. Cells were then stained for cell surface marker expression by flow cytometry. WT31 and OKT3 stainings were used as negative and positive controls, respectively (11).

NANAse (Sigma) treatments were done as described (12). NANAse effects were controlled externally by the increased WT31 binding of a γδ$^+$ T cell line termed Peer (data not shown) and internally by the decreased binding of a CD43-specific antibody, as described (13).

Blue Native (BN)-PAGE and Western Blotting—Published methods were used for the two-step affinity purification of the TCR (14). Briefly, cells were stimulated with pervanadate and lysed with 1% digitonin lysis buffer containing sodium orthovanadate. Phosphorylated proteins were purified with 1 μg of 4G10 and 3 μl of protein G-Sepharose, washed three times, and subsequently eluted in BN buffer (500 mM ε-aminocaproic acid, 20 mM NaCl, 10% glycerol, 2 mM EDTA, and 20 mM bis-Tris, pH 7) including 50 mM phenylphosphate, 1 unit of alkaline phosphatase, and 1% digitonin. Dephosphorylated TCRs were separated by BN-PAGE as described (15). Western blots were developed with the anti-ζ antiserum 448. Ferritin monomers (f1; 400 kDa), dimers (f2; 880 kDa), and trimers (f3; 1320 kDa) were included as molecular mass standards. Under these conditions, the normal dephosphorylated $\alpha\beta\gamma\epsilon\delta\epsilon\zeta_2$ TCR·CD3 runs at ~400 kDa (f1) despite the fact that the relative molecular masses of the isolated dimers add up to only 230 kDa (90 + 50 + 50 + 40). Therefore, shape as well as molecular mass is important in BN-PAGE gels. For antibody-based gel shift experiments, samples were pre-incubated with βF1 (TCRβ) mAb or Fab fragments of SP34 (CD3ε) before electrophoresis. A detailed description and analysis of the wild-type TCR by BN-PAGE has been submitted.[2]

RESULTS

CD4$^+$ and CD8$^+$ CD3γ-deficient T Lymphocytes Express Biochemically Different Membrane αβ TCR·CD3 Complexes—Natural CD3γ-deficient (γ$^-$) T cells were biotinylated or radioiodinated, lysed, and immunoprecipitated with CD3-specific as well as with TCR-specific mAb and compared with normal controls (γ$^+$). The results showed that, in contrast to biosynthetic experiments, the amount of surface CD3-associated TCR (and ζ) proteins was very low in γ$^-$ cells (Fig. 1*A*). This precluded a meaningful analysis of the TCR composition of the complex by this method. We have previously reported by immunoprecipitation that surface CD3δ from CD8$^+$ γ$^-$ cells showed an impaired electrophoretic mobility in comparison with controls because of its abnormal glycosylation (Fig. 1*A*, *right*). This finding correlated with complete endo-β-*N*-acetylglucosaminidase H resistance (6). Therefore, we next analyzed the CD3δ from CD4$^+$ γ$^-$ cells. The results demonstrated that, in contrast to CD8$^+$ γ$^-$ cells, the CD3δ from CD4$^+$ γ$^-$ cells was similar to that from controls, both in terms of relative mobility and endo-β-*N*-acetylglucosaminidase H sensitivity (Fig. 1*B*). The direct immunoprecipitation of TCR chains showed that CD4$^+$ γ$^-$ cells were comparable with CD4$^+$ γ$^+$ cells in terms of TCR chain composition, whereas CD8$^+$ γ$^-$ cells clearly lacked normal surface TCRα and TCRβ chains (Fig. 2). These differences were TCR-specific, because control immunoprecipitates of major histocompatibility complex class I molecules were equivalent in all cells.

To further characterize the surface TCR chains of the mutant cells, immunofluorescence confocal analyses were performed using the same mAb. Expression of the CD4 or CD8 coreceptors was used as a positive or negative control in each cell type. The results indicated that both TCRα and TCRβ chains showed normal (mostly surface) distribution and fluorescence intensities in CD4$^+$γ$^-$ lymphocytes (Fig. 3). CD8$^+$γ$^-$

---

[2] W. W. A. Schamel and B. Alarcón, submitted for publication.

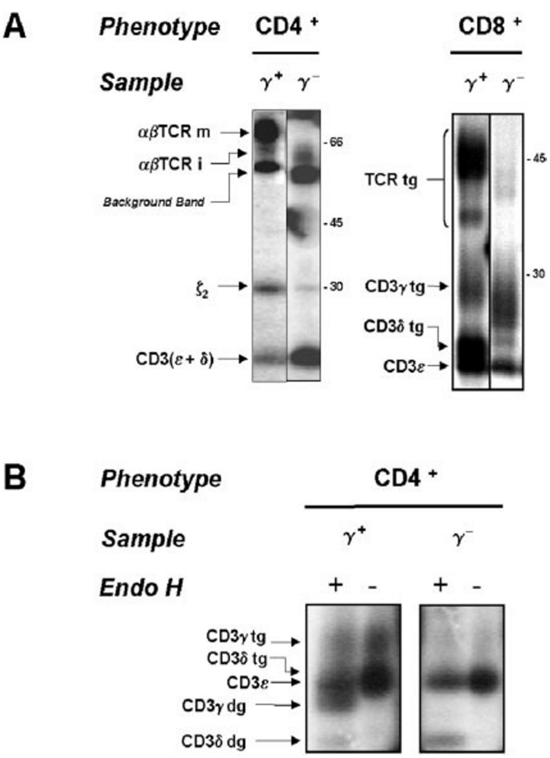

FIG. 1. **Immunoprecipitation of surface-labeled αβTCR·CD3 from CD3γ-deficient CD4$^+$ and CD8$^+$ T cells.** *A*, at least 5 × 10^6 γ^+ and γ^- cells/lane, either CD4$^+$ or CD8$^+$, were surface-labeled and lysed with biotin/digitonin or ^{125}I/Brij96, respectively, and precipitated with a CD3-specific mAb before electrophoresis under reducing (*right*) or non-reducing (*left*) conditions in 10% polyacrylamide gels. Note that CD3γ is poorly labeled by biotin. *B*, 5–10 × 10^6 CD4$^+$ γ^+ and CD4$^+$ γ^- cells/lane were surface-labeled, lysed in 1% digitonin-containing buffer, and digested, where indicated, with endo-β-*N*-acetylglucosaminidase H (*Endo H*) before electrophoresis under reducing conditions in 10% polyacrylamide gels. Positions of the expected normal proteins are indicated (*tg*, totally glycosylated; *dg*, deglycosylated). *αβTCRm* and *αβTCRi* denote the mature or immature forms of the heterodimer, respectively. TCR denotes the monomeric forms of the TCR (α or β) chains.

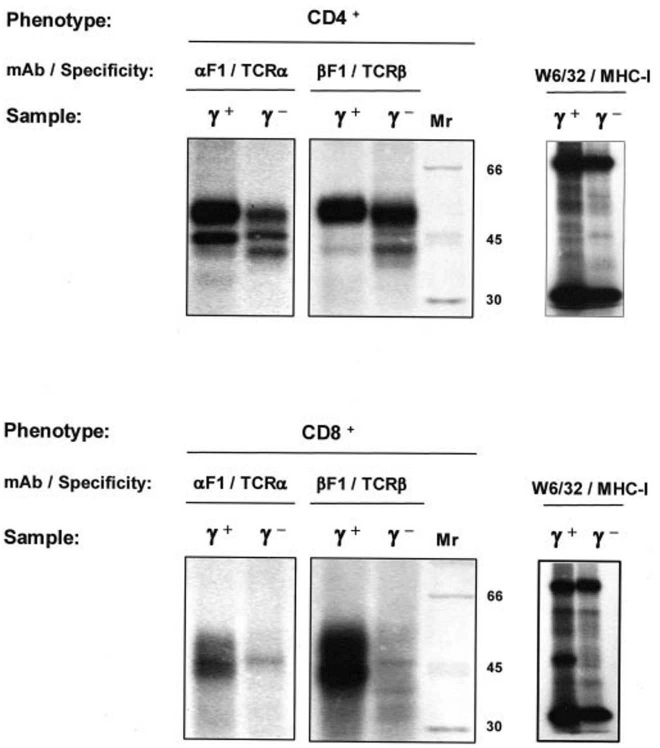

FIG. 2. **Immunoprecipitation of surface-iodinated TCR chains from CD3γ-deficient CD4$^+$ and CD8$^+$ T cells.** Equal numbers of γ^+ and γ^- cells, either CD4$^+$ or CD8$^+$, were surface-labeled with ^{125}I, lysed in 1% Nonidet P-40-containing buffer, and precipitated with a TCR-specific mAb (*W6/32*) or, as a control, a major histocompatibility complex-specific mAb (*MHC-1*) before electrophoresis under reducing conditions in 10% polyacrylamide gels.

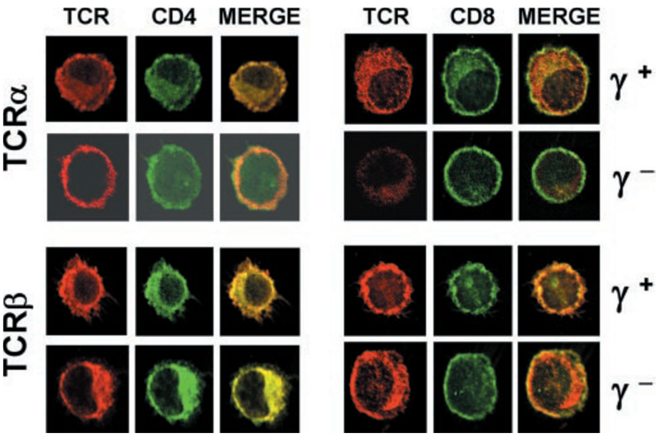

FIG. 3. **Confocal analysis of TCRα and TCRβ expression by CD3γ-deficient CD4$^+$ and CD8$^+$ T cells.** 2.5 × 10^4 CD4$^+$ or CD8$^+$ cells, both γ^+ and γ^-, were cytocentrifuged, acetone-fixed, and stained with purified TCRα- and TCRβ-specific mAbs and Cy3-conjugated secondary antibodies. CD4- and CD8-fluorescein isothiocyanate stainings were included as a positive control. Cy3 and fluorescein isothiocyanate emissions were acquired simultaneously. The images show a medial optical cut of representative cells. CD4 staining was intracellular in this particular preparation.

cells also showed normal expression of TCRβ by this assay, but TCRα was hardly detectable and, when present (10–20% of cells), mostly intracellular. The discrepancy in TCRβ expression by CD4$^+\gamma^-$ cells between these data and the immunoprecipitation results (above) may be due to technical differences, such as the use of acetone for confocal analysis.

In a last set of experiments, the native surface TCR·CD3 complexes from CD4$^+$ and CD8$^+$ mutant cells were compared (14, 15). The results indicated that the TCR·CD3 complex from CD4$^+$ γ^- T lymphocytes was similar to normal complexes from γ^+ T cells (CD4$^+$, CD8$^+$, or Jurkat), although with delayed electrophoretic mobility (Fig. 4*A*). This observation was compatible with either a different stoichiometry or a different structure (such as glycosylation or conformation changes) of the mutant complex (see "Experimental Procedures"). To distinguish between these two possibilities, antigenic shift experiments were performed. One shift indicates that there is a single chain per complex, and two shifts denote two binding sites per complex. The results indicated that the mutant TCR·CD3 complex had a normal stoichiometry when compared with that of γ^+ T cells (Jurkat, Fig. 4*B*, or PBL, not shown). It contained one TCRβ chain (hence a single αβ heterodimer) and two CD3ε chains (probably representing two CD3δε dimers, because γ was absent). In summary, these experiments support an $\alpha\beta(\delta\epsilon)_2\zeta_2$ model for the mutant TCR·CD3 complex in CD4$^+$ γ^- cells, where the γε dimer is replaced by the analogous δε dimer. Therefore, other types of modifications, such as glycosylation or conformation, may explain the delayed migration of the mutant complex. In sharp contrast, CD8$^+$ γ^- cells expressed a very different TCR·CD3 complex as compared with their CD4$^+$ γ^- counterparts. Native TCR·CD3 complexes isolated from CD8$^+$ γ^- cells migrated along a broad smear, suggesting the existence of a heterogeneous population of complexes in these cells (Fig. 4*A*). The stoichiometry of these heterogeneous TCR·CD3 complexes could not be determined by antigenic shift due to the basal broad smear.

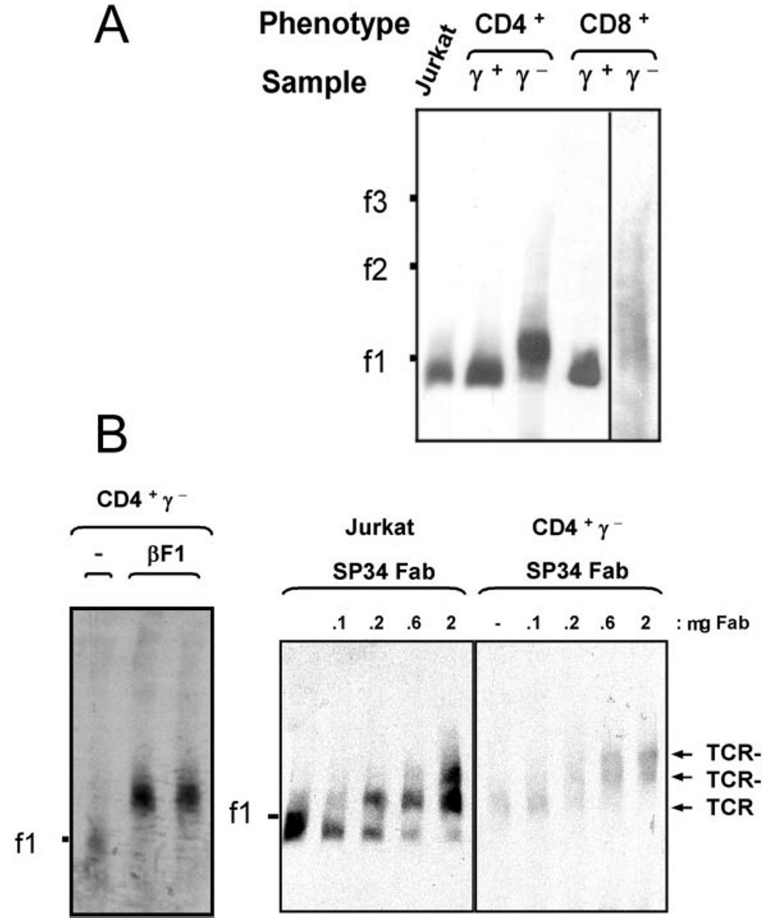

FIG. 4. **Native surface TCR·CD3 complex analyses of CD3γ-deficient CD4$^+$ and CD8$^+$ T cells**. *A*, equal numbers of γ^+ and γ^- cells, either CD4$^+$ or CD8$^+$, were stimulated with pervanadate and lysed in 1% digitonin before the purification of phosphorylated proteins using anti-phosphotyrosine-immunoprecipitation. Bound proteins were eluted, dephosphorylated, and separated by BN-PAGE. Western blots were developed with anti-ζ. Ferritin monomers (*f1*), dimers (*f2*), and trimers (*f3*) were included as molecular weight standards. *B*, antibody-based gel shift assay of CD4$^+$ γ^- or Jurkat T cells using the indicated mAbs.

From these studies we conclude that CD4$^+$ γ^- and CD8$^+$ γ^- cells shared a poor surface association of CD3 to TCR chains. We also conclude, by using several experimental approaches, that their surface αβ TCR·CD3 complexes differed biochemically in the CD3 and the TCR components, as well as in the complete native complex.

CD4$^+$ and CD8$^+$ Primary T Lymphocytes Express Biochemically Different Membrane αβ TCR·CD3 Complexes—Normal primary CD4$^+$ T cells show higher TCR·CD3 staining levels than do CD8$^+$ cells (~1.5-fold with OKT3; Ref. 2). This difference was interpreted as quantitative under the assumption that the αβ TCR·CD3 complex is identical in both cell types. However, as shown above and in Ref. 6, the analysis of γ^- TCR·CD3 complexes suggested the existence of hitherto unrecognized structural differences between both cell lineages. These results prompted us to search for qualitative αβ TCR·CD3 complex differences in normal CD4$^+$ and CD8$^+$ primary T lymphocytes. To test this hypothesis, a broad epitopic scan of the TCR·CD3 complex was performed by three-color flow cytometry using several CD3- or TCR-specific mAbs within gated CD4$^+$ and CD8$^+$ subsets. To exclude CD8$^+$ NK cells (mostly CD8$\alpha\alpha^+$, which stain dull for CD8 mAb), only CD8$^{\mathrm{bright}}$ cells (CD8$\alpha\beta^+$ T cells) were analyzed. As a control, CD18-specific mAbs were used, which stained primary CD4$^+$ and CD8$^+$ T cells similarly. The data are depicted in Fig. 5*A* as MFI ratios of each mAb in CD4$^+$ relative to CD8$^+$ T cells, with representative histograms in Fig. 5*B*. The results showed that, for most of the mAb assayed, CD4$^+$ lymphocytes stained better (MFI ratio >1.5, Fig. 5*A*) than did CD8$^+$ lymphocytes, as described (2). However this was not the case with two mAbs that stained CD8$^+$ T cells similarly (MFI ratio = 1.2, WT31; Ref. 16) or even better (MFI ratio <1, RW2-8C8; Ref. 17) than did CD4$^+$ T cells. These observations are not consistent with the quantitative interpretation but, rather, with the existence of conformational (*i.e.* qualitative) differences in the αβ TCR·CD3 complex between CD4$^+$ and CD8$^+$ T cells.

To determine whether these conformational differences were developmentally regulated or regulated by activation (as described for activated γδ T cells, 18), mature CD4$^+$ and CD8$^+$ T lymphocytes were analyzed and compared for CD3 (and CD18) expression in four consecutive differentiation stages as follows: 1) intrathymic single positive (CD4$^+$CD8$^-$ or CD4$^-$CD8$^+$) early mature T cells (gated as described under "Experimental Procedures"); 2) peripheral blood naïve T cells (defined by CD45RA$^+$ expression, which identifies recent thymic emigrants, Ref. 19); 3) peripheral blood memory T cells (CD45RO$^+$); and 4) recently activated peripheral blood T cells (gated as CD69$^+$ after phytohemagglutinin incubation) or constitutively activated *H. saimiri* (HVS)-transformed T cells (20). The results indicated that the increased RW2-8C8 binding of CD8$^+$ as compared with that of CD4$^+$ T cells was essentially independent of their activation or differentiation status, although it was more apparent in peripheral T cells (naïve, memory, or activated) than in intrathymic single positive T cells (Fig. 5*C*). In contrast, increased UCHT1 binding of CD4$^+$ T cells as compared with that of CD8$^+$ T cells was clearly regulated by activation and differentiation, as it occurred only in intrathymic and naïve T cells but not in memory or activated T cells. These changes were specific for the TCR·CD3 complex, as CD18 was regulated in an opposite fashion. Interestingly, equivalent UCHT1 binding of CD4$^+$ and CD8$^+$ memory T cells was acquired through both a decreased binding of CD4$^+$ T cells and an increased binding of CD8$^+$ T cells relative to their naïve counterparts, whereas RW2-8C8 binding differences were unaltered by the naïve/memory transition (not shown). Therefore, CD4$^+$ and CD8$^+$ T cells indeed regulated their αβ TCR·CD3 conformational differences but did so differently for each epitope, and the RW2-8C8 epitope was well conserved along mature T cell differentiation.

It has been proposed that lipid raft integrity affects the topological arrangement of the TCR·CD3 complex on the cell surface (10). Also, it is believed that a fraction of TCR·CD3 is raft-associated because of its association with the cytoplasmic portion of the CD8 (or CD4) coreceptor (21). We therefore reasoned that the conformational TCR·CD3 differences observed between $CD4^+$ and $CD8^+$ T cells could be due, at least in part, to the differential arrangement of lipid raft-associated surface TCR·CD3 clusters or arrays. To test this hypothesis, primary T lymphocytes were treated with MβCD and analyzed for CD3 expression within the $CD4^+$ and $CD8^{bright}$ T cell subsets using several TCR·CD3-specific mAbs (Fig. 5, *D* and *E*). MβCD disrupts lipid microdomains by extracting cholesterol from plasma membranes (22). WT31 and OKT3 were used as negative and positive controls for the TCR·CD3 complex, respectively, as described (11). Two different CD18-specific mAbs were used as additional negative controls (10). The result showed that the TCR·CD3 complex was more dependent on lipid raft integrity in $CD8^+$ as compared with $CD4^+$ T cells when probed with several antibodies (RW2-8C8, OKT3, Leu4, Cris7, UCHT1, and BMA031) but not with WT31 (as expected; Ref. 11). These results are consistent with the existence of more lipid raft-associated TCR·CD3 domains (or isoforms) in $CD8^+$ than in $CD4^+$ T cells. Interestingly, RW2-8C8 seemed to bind a relatively lipid raft-independent TCR·CD3 epitope (or isoform) in $CD4^+$, which was lipid raft-dependent in $CD8^+$ T cells. It was surprising to find that the lipid raft-dependent TCR·CD3-specific mAbs were those that bound $CD4^+$ better than $CD8^+$ T cells (compare Fig. 5, *A* and *D*).

Because the TCR·CD3 protein components are equivalent in $CD8^+$ and $CD4^+$ T cells, it was also possible that the conformational differences were due, in part, to glycosylation variability of the TCR·CD3 complex, as shown for γδ T cells (12, 18). To test this hypothesis, primary T cells were digested with NANAse and analyzed for CD3 expression within the $CD4^+$ and $CD8^{bright}$ T cell subsets using RW2-8C8 and Leu4 (Fig. 6*A*). Decreased binding of CD43 was used as an internal control of NANAse treatment, as described (13). The results showed that NANAse-treated $CD4^+$ T cells became indistinguishable from $CD8^+$ T cells using RW2-8C8 but not Leu4, suggesting that NANA-associated glycosylation of the TCR·CD3 components in $CD4^+$ T cells partially hides (or builds) the RW2-8C8 epitope.

To further characterize the RW2-8C8 epitope, competition experiments were performed on several mature and immature T lymphocyte types using phycoerythrin-labeled Leu4 (CD3-specific) or BMA031 (framework TCRαβ-specific). The results

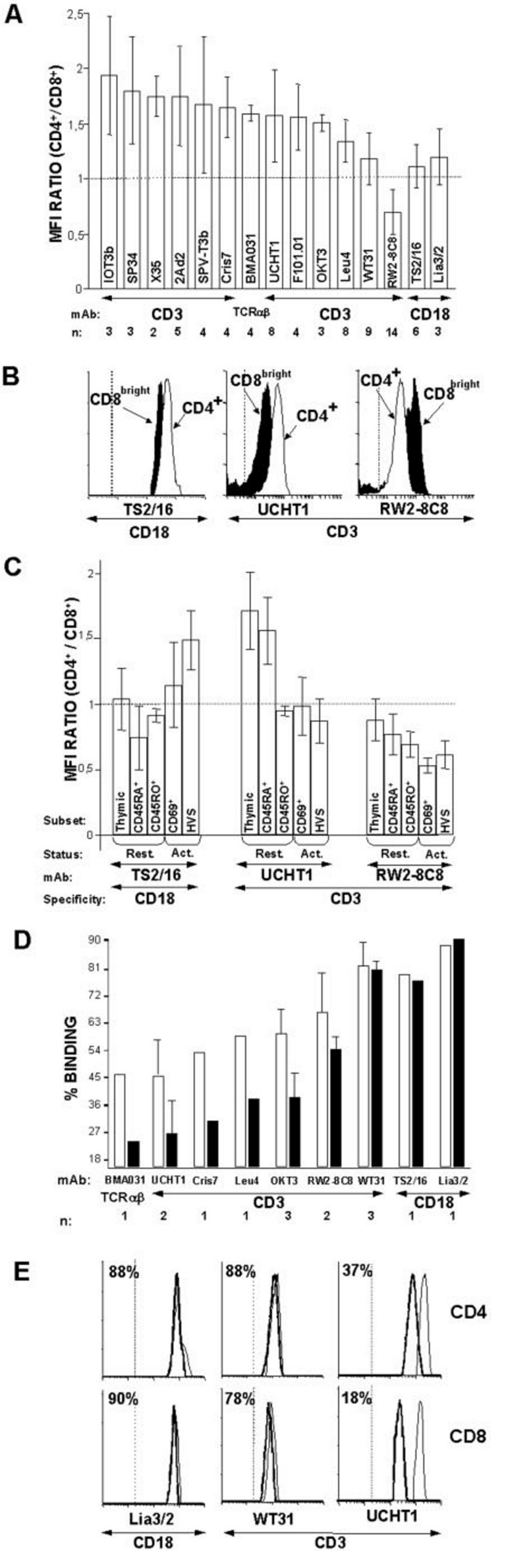

FIG. 5. **Comparative cell surface TCR·CD3 expression by normal $CD4^+$ and $CD8^+$ peripheral blood lymphocytes and dependence on lipid raft integrity**. *A*, MFI ratios ± S.D. of $CD4^+$ relative to $CD8^+$ T cells with the indicated mAb in *n* independent donors. MFI ratios above or below 1 (indicated by the *horizontal dotted line*) reflect an increased or decreased mAb binding to $CD4^+$ cells, respectively. As an invariant control, CD18/CD11b expression was evaluated in parallel with two different mAbs recognizing different epitopes of the same molecule. *B*, representative reactivity patterns of selected mAbs in $CD4^+$ (*open histograms*) and $CD8^{bright}$ (*filled histograms*) PBLs. Profiles are shown as the logarithm of relative fluorescence *versus* the number of cells. The *vertical line* in each panel indicates the upper limit of background fluorescence using isotype-matched irrelevant mAb. *C*, MFI ratios as in *panel A* for the indicated mAb and T cell subsets from at least three independent donors (*HVS*, *H. saimiri*-transformed; *Rest*, resting; *Act*, activated). *D*, purified PBLs from *n* independent donors were treated with MβCD to disrupt rafts and analyzed for surface binding of the indicated mAbs within $CD4^+$ and $CD8^+$ T cell subsets. The results are given relative to untreated cells. *E*, representative reactivity patterns of selected mAbs in $CD4^+$ and $CD8^{bright}$ PBLs before (*thin histograms*) or after (*thick histograms*) MβCD treatment. The numbers denote the percentage of binding as in *panel D*.

(Fig. 6*B*) showed that preincubation with unlabeled RW2-8C8 blocked BMA031 but not Leu4 (or UCHT1, not shown) binding. In contrast, another CD3-specific mAb (UCHT1) or an irrelevant mAb (CD18) did not preclude BMA031 binding. However, RW2-8C8 is CD3- rather than TCRαβ-specific, as it was shown to bind TCRγδ$^+$ BMA031$^-$ PBLs (Fig. 6*B*, *bottom right*). Therefore, RW2-8C8 binds to a CD3 determinant that is closer to (or more influenced by mAb binding to) the BMA031 epitope than to the Leu4 or UCHT1 epitopes. Alternatively, these results are consistent with the existence of two isoforms of surface TCR·CD3 complexes, one that cannot be engaged by Leu4 or BMA031 if RW2-8C8 is present and another in which RW2-8C8 binding blocks BMA031 but not Leu4 or UCHT1 binding. Primary CD4$^+$ and CD8$^+$ γ$^-$ T lymphocytes were also analyzed for the expression of the epitope recognized by RW2-8C8. The results (Fig. 6*C*) indicated that RW2-8C8 but not Leu4 again stained CD8$^+$ T cells better than it stained CD4$^+$ T cells even when CD3γ is absent. These results demonstrated that RW2-8C8 binds to a CD3 determinant that is more strongly expressed by CD8$^+$ than by CD4$^+$ T cells even in the absence of CD3γ. The notion that RW2-8C8 may be detecting a distinct CD3 conformational epitope was explored in several T-lineage cell types as follows: 1) a cell line expressing the pre-TCR·CD3, an immature BMA031$^-$ TCR·CD3 complex in which the variable TCRα chain is replaced by the invariant pTα component (SupT1; Ref. 23); 2) Jurkat cells bearing the mature BMA031$^+$ TCRαβ; and 3) CD4$^+$CD8$^+$ (double positive) thymocytes bearing an immature BMA031$^+$ TCRαβ (24). The results (Fig. 6*D*) showed that RW2-8C8 was the best CD3 antibody in terms of SupT1 or double positive thymocyte binding, but not for the conventional TCR·CD3 expressed by control Jurkat T cells. Taken together, these results indicated that RW2-8C8 binds to a peculiar CD3 determinant that is close to the TCR heterodimer, more prominent than those recognized by other CD3-specific mAb in immature TCRβ-containing ensembles, and more strongly expressed by CD8$^+$ than by CD4$^+$ T cells even when CD3γ is absent.

Finally, surface radioiodination and immunoprecipitation studies using both CD3-and TCR-specific mAbs were performed to compare the TCR·CD3 expressed by purified primary CD4$^+$ and CD8$^+$ T cells. The results (Fig. 7) again revealed the existence of consistent differences in TCR (but not CD3) components between CD4$^+$ and CD8$^+$ T cells. The densitometry ratio of high to low molecular weight forms of αβTCR (*TCRtg* (tg, totally glycosylated) in Fig. 7) was higher in CD4$^+$ T cells than in CD8$^+$ T cells (1.8 *versus* 1.4, 2.5 *versus* 1.6. and 1.7 *versus* 1.4 using CD3-, TCRβ-, or TCRα+TCRβ-specific mAbs, respectively). These differences are probably due to *N*-linked glycosylation trimming, because they disappeared after canase treatment.

DISCUSSION

Lineage-associated αβTCR·CD3 Variation—In the present report, we showed by several experimental approaches that CD4$^+$ and CD8$^+$ mature T lymphocytes do not express identical surface αβTCR·CD3 complexes. First, CD3γ-deficient CD4$^+$ and CD8$^+$ T cells were shown to differ by the following three criteria: 1) CD3δ chain glycosylation (Fig. 1 and Ref. 6);

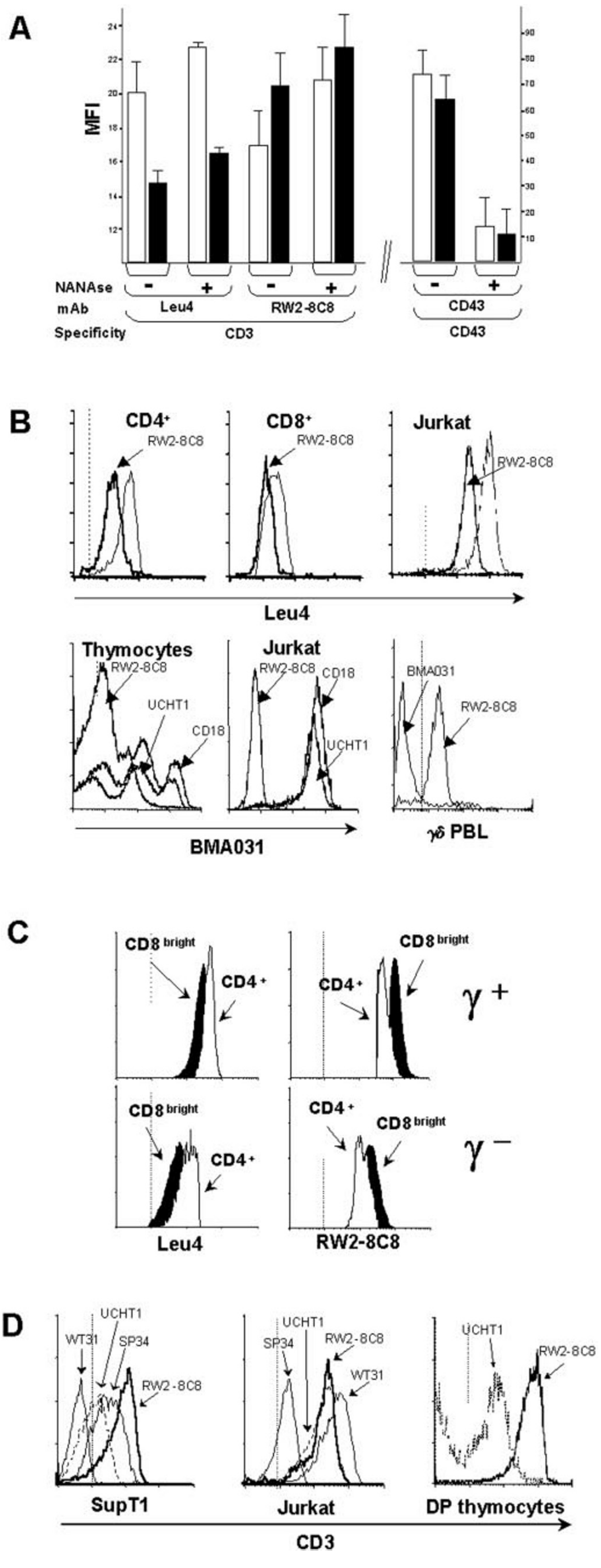

FIG. 6. **Characterization of the RW2-8C8 antibody.** *A*, purified PBLs from normal donors were NANAse-treated (+) to remove sialic acid residues or left untreated (−) and analyzed for surface binding of RW2-8C8, Leu4, and CD43 (positive control) within CD4$^+$ and CD8$^+$ T cell subsets. *B*, mature or immature T cells were stained with Leu4-phycoerythrin (or UCHT1, not shown) or BMA031-phycoerythrin before (*thin histograms*) or after (*thick histograms*) preincubation with unlabeled RW2-8C8, CD18, or UCHT1. Gated TCRγδ$^+$ PBL reactivity patterns with BMA031 and RW2-8C8 are shown to illustrate that only the latter is CD3-specific (*bottom right*). *C*, representative reactivity patterns of RW2-8C8 (*right*) and Leu4 (*left*) in γ$^-$ CD4$^+$ (*open histograms*) and CD8^{bright} (*filled histograms*) peripheral blood lymphocytes. *D*, comparative reactivity patterns of several mAbs with SupT1 (pTαβTCR$^+$), Jurkat (αβTCR$^+$), and CD4$^+$CD8$^+$ (DP) thymocytes (immature αβTCR$^+$).

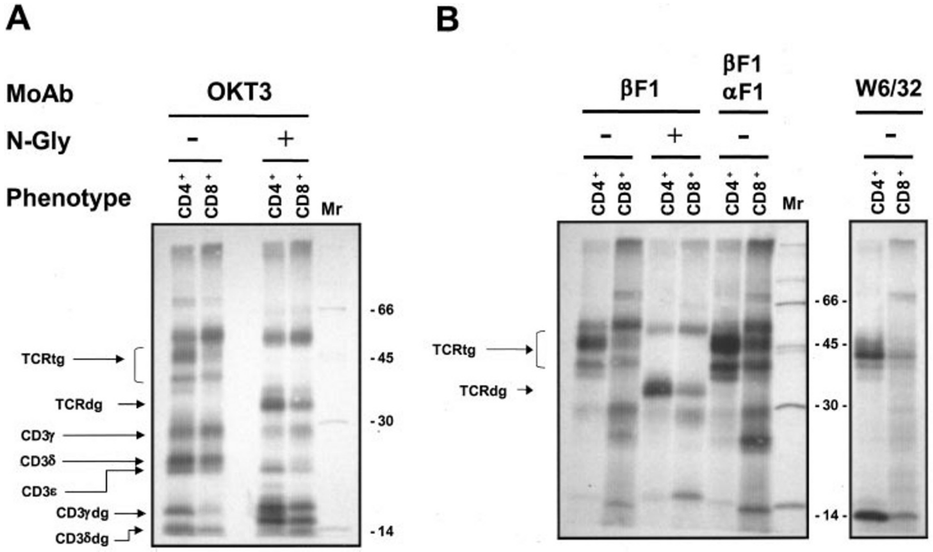

FIG. 7. **Immunoprecipitation of surface-iodinated TCR·CD3 complexes from isolated $CD4^+$ and $CD8^+$ fresh peripheral blood lymphocytes**. $CD4^+$ (15×10^6 cells) and $CD8^+$ (5×10^6 cells) PBLs from a normal donor were immunomagnetically isolated, surface-labeled with ^{125}I, lysed in 1% digitonin-containing buffer, precipitated with the indicated CD3-, TCR-, or HLA-specific mAb, and digested, where indicated (+), with *N*-glycosidase F (*N-Gly*) before electrophoresis under reducing conditions in 10% polyacrylamide gels. The positions of the expected TCR and CD3 proteins are indicated (*dg*, deglycosylated; *tg*, totally glycosylated).

2) TCRα and TCRβ chain content (Fig. 2 and 3; and 3) native αβTCR·CD3 migration (Fig. 4). Second, primary normal $CD4^+$ and $CD8^+$ T cells were shown to express conformationally and biochemically different surface αβTCR·CD3 complexes (Figs. 5 and 7, respectively), which were regulated by activation and differentiation for certain epitopes, likely due to lipid raft-dependent arrangements or glycosylation. These results confirm our previous biosynthetic and phenotypic studies in CD3γ-deficient T cells (6) and extend the observations to primary T lymphocytes from normal individuals. Biosynthetic studies showed that $CD8^+$ but not $CD4^+$ CD3γ-deficient T cells contained a small αβ heterodimer composed of abnormally glycosylated TCRβ and an abnormally small CD3-associated chain that was not recognized by TCRα-specific antibodies. However, the TCR Cα gene was normal, and the atypical 32-kDa TCRα observed intracellularly was indeed shown to be TCRα by protein sequencing using matrix-assisted laser desorption ionization time-of-flight (data not shown).

The TCR·CD3 complex is a very flexible structure. For instance, the γδ TCR (and γδ T cell development) can be quite CD3δ-independent in mice (5, 25). There are descriptions of CD3-specific mAb that do not bind the γδ TCR·CD3 complex unless it was deglycosylated previously (WT31, 12), and even T cell activation can modify CD3γ glycosylation (18) with clear biochemical consequences. Similarly, αβTCR·CD3 expression is possible without CD3γ (4, 8) or δ (5), but not without both (26). Therefore, it is not surprising that further flexibility is present in $CD4^+$ *versus* $CD8^+$ T cells, particularly when CD3γ is absent, but also in normal donors. The mAbs used for surface TCR·CD3 detection were obtained using different antigens (bulk PBL or thymocytes, purified primary T cells or T cell lines, solubilized cell membranes, purified TCR·CD3 proteins, etc.) and different screening criteria (fresh, fixed, or tumor T cell binding, cytolysis blocking, PBL stimulation, etc.) (27). Therefore, a possible explanation for the observed lineage-specific binding differences could stem from the immunization or screening criteria used in each case, a situation that would favor naïve $CD4^+$ and lipid raft-dependent over naïve $CD8^+$ and lipid raft-independent TCR·CD3 binding with certain mAbs. These differences could be exploited for therapeutic purposes, such as lineage-specific immunosuppression during graft rejection.

What could be the mechanism responsible for the observed lineage-dependent biochemical TCR·CD3 differences? Because all of the subunits are present in both cases (even with the same stoichiometry, if isolated with digitonin), we believe that there must be biochemical differences in the way the complex is assembled, glycosylated, trimmed, or topologically arranged in the cell surface in each T cell subset after the lineage decision is reached and apparently also upon antigen recognition (28). The reported physical association of CD3δ with the raft-resident coreceptor molecules CD4 and CD8 on resting T lymphocytes could contribute to the observed differences (21, 29). In addition, the individual TCR·CD3 subunits could possess slightly distinct structures. These differences could be caused by developmentally acquired fundamental changes that distinguish the two cell types, including the glycosylation machinery (30, 31) or chaperones. For instance, the inactivation of a sialyltransferase (ST3Gal-I) strongly reduced peripheral $CD8^+$ but not $CD4^+$ cell numbers (32). Further work is required to address this issue, perhaps through a comparative genomic approach that includes the chaperones and enzymes involved in glycosylation pathways. Interestingly, TCR·CD3 signaling capacity and dynamics are not affected by the observed biochemical differences, either with or without CD3γ (6–8), further suggesting that the changes are required for optimal receptor-coreceptor *cis* interactions during antigen recognition and signal transduction in each cell type (33). An alternative interpretation is that two different TCR populations exist on the cell membrane and that their relative proportions change in different T cell subsets. Antibodies such as RW2-8C8 may detect those changes.

αβTCR·CD3 Structure and Function—The results are consistent with a recent report on the structure and stoichiometry of the TCR·CD3 complex *in vitro* (34). The authors demonstrated that CD3γ is important for incorporation of ζ but not ε to the complex, as shown in Fig. 1*A* (CD3-associated ζ is very scarce in γ^- cells) and in Ref. 6. They also proved that, whereas TCRα is strictly associated to δε dimers, TCRβ can interact with γε as well as with δε dimers. This apparent biochemical promiscuity may explain why surface TCR·CD3 adopts a $\alpha\beta(\delta\epsilon)_2\zeta_2$ stoichiometry (Fig. 4) and why its expression is so notable despite the lack of CD3γ (7). Although the same authors showed that isolated αβ and δε dimers do not normally assemble into $\alpha\beta(\delta\epsilon)_2$ complexes *in vitro*, intrathymic selection mechanisms may expand, *in vivo*, the otherwise rare T cell precursors that manage to assemble a viable surface TCR·CD3 complex with such stoichiometry. *In vivo* observations further support this contention, because human CD3γ-deficient individuals showed significant T cell development with only mild lymphopenia and immunodeficiency, whereas CD3δ-deficient patients had no T cells and very severe clinical abnormalities (35).

Acknowledgments—We greatly appreciate the generous supply of rIL2 from Dr. Craig W. Reynolds (Frederick Cancer Research and Development Center, NCI, National Institutes of Health, Frederick, MD) and the technical help provided at our university by Dr. A. Alvarez-Barrientos of the Central Cytometry Facility (confocal studies), Dr. A. Varas of the Department of Cell Biology (cytospins), and B. Fernández of the Department of Immunology (cell cultures). We also thank the Pediatric Cardiosurgery Units from Centro Especial Ramón y Cajal and Ciudad Sanitaria La Paz (Madrid) for the thymus samples and the mAb donors cited under "Experimental Procedures."

REFERENCES

1. Alarcon, B., Gil, D., Delgado, P., and Schamel, W. W. (2003) *Immunol. Rev.* **191,** 38–46
2. Thibault, G., and Bardos, P. (1995) *J. Immunol.* **154,** 3814–3820
3. Timón, M., Arnaiz-Villena, A., Rodríguez-Gallego, C., Pérez-Aciego, P., Pacheco, A., and Regueiro J. R. (1993) *Eur. J. Immunol.* **23,** 1440–1444
4. Haks, M. C., Krimpenfort, P., Borst, J., and Kruisbeek, A. M. (1998) *EMBO J.* **17,** 1871–1882
5. Dave, V. P., Cao, Z., Browne, C., Alarcón, B., Fernández-Miguel, G., Lafaille, J., de la Hera, A., Tonegawa, S., and Kappes D. J. (1997) *EMBO J.* **16,** 1360–1370
6. Zapata, D. A., Pacheco-Castro, A., Torres, P. S., Ramiro, A. R., San José, E., Alarcón, B., Alibaud, L., Rubin, B., Toribio, M. L., and Regueiro, J. R. (1999) *J. Biol. Chem.* **274,** 35119–35128
7. Torres, P. S., Alcover, A., Zapata, D. A., Arnaud, J., Pacheco, A., Martin-Fernandez, J. M., Villasevil, E. M., Sanal, O., and Regueiro J. R. (2003) *J. Immunol.* **170,** 5947–5955
8. Pacheco-Castro, A., Alvarez-Zapata, D., Serrano-Torres, P., and Regueiro J. R. (1998) *J. Immunol.* **161,** 3152–3160
9. Lim, L. C., Fiordalisi, M. N., Mantell, J. L., Schmitz, J. L., and Folds, J. D. (1998) *Clin. Diagn. Lab. Immunol.* **5,** 392–398
10. Drake, D., III, and Braciale T. (2001) *J. Immunol.* **166,** 7009–7013
11. Uhlin, M., Masucci, M., and Levitsky V. (2003) *Scand. J. Immunol.* **57,** 99–106
12. van de Griend, R. J., Borst, J., Tax, W. J., and Bolhuis, R. L. (1988) *J. Immunol.* **140,** 1107–1110
13. Borche, L., Lozano, F., Vilella, V., and Vives, J. (1987) *Eur. J. Immunol.* **17,** 1523–1526
14. Schamel, W. W. A., and Reth M. (2000) *Immunity* **13,** 5–14
15. Schägger, H., and Jagow, G. (1991) *Anal. Biochem.* **199,** 223–231
16. Spits, H., Borst, J., Tax, W., Capel, P. J., Terhorst, C., and de Vries J. E. (1985) *J. Immunol.* **135,** 1992–1998
17. Meuer, S. C., Hodgdon, J. C., Hussey, R. E., Protentis, J. P., Schlossman, S. F., and Reinherz E. L. (1983) *J. Exp. Med.* **158,** 988–993
18. Hayes, S. M., Laky, K., El Khoury, D., Kappes, D. J., Fowlkes, B. J., and Love P. E. (2002) *J. Exp. Med.* **196,** 1355–1361
19. Mackall, C. L., Granger, L., Sheard, M. A., Cepeda R., and Gress R. E. (1993) *Blood* **82,** 2585–2594
20. Meinl E., Hohlfeld, R., Wekerle, H., and Fleckenstein B. (1995) *Immunol. Today* **16,** 55–58
21. Doucey, M. A., Goffin, L., Naeher, D., Michielin, O., Baumgartner, P., Guillaume, P., Palmer, E., and Luescher, I. F. (2003) *J. Biol. Chem.* **278,** 3257–3264
22. Hartel, S., Diehl, H., and. Flavo O. (1998). *Anal. Biochem.* **258,** 277
23. Carrasco, Y. R., Ramiro, A. R., Trigueros, C., de Yebenes, V. G., García-Peydro, M., and Toribio, M. L. (2001) *J. Exp. Med.* **193,** 45–58
24. Finkel, T. H., McDuffie, M., Kappler, J. W., Marrack, P., and Cambier, J. C (1987) *Nature* **330,** 179–181
25. Hayes, S. M., and Love, P. E. (2002) *Immunity* **16,** 827–838
26. Malissen, B., Ardouin, L., Lin, S. Y., and Malissen, M. (1999) *Adv. Immunol.* **72,** 103–148
27. Yokoyama W. M (1991) in *Current Protocols in Immunology* (Coligan, J. E., Kruisbeek, A. M., Margulies, D. H., Shevach, E. M., and Trober, W.) pp. 2.5.1-2.5.17, Greene Publishing and Wiley Interscience, New York
28. Daniels, M. A., Hogquist, K. A., and Jameson, S. C. (2002) *Nat. Immunol.* **3,** 903–910
29. Suzuki, S., Kupsch, J., Eichmann, K., and Saizawa, M. K. (1992) *Eur. J. Immunol.* **22,** 2475–2479
30. Daniels, M. A., Devine, L., Miller, J. D., Moser, J. M., Lukacher, A. E., Altman, J. D., Kavathas, P., Hogquist, K. A., and Jameson S. C. (2001) *Immunity* **15,** 1051–1061
31. Moody, A. M., Chui, D., Reche, P. A., Priatel, J. J., Marth, J. D., and Reinherz, E. L (2001) *Cell* **107,** 501–512
32. Priatel, J. J., Chui, D., Hiraoka, N., Simmons, C. J. T., Richardson, K. B., Page, D. M., Fukuda, M., Varki, N. M., and Marth, J. M. (2000) *Immunity* **12,** 273–283
33. Garcia, K. C., Scott, C. A., Brunmark, A., Carbone, F. R., Peterson, P. A., Wilson, I. A., and Teyton, L. (1996) *Nature* **384,** 577–581
34. Call, M. E., Pyrdol, J., Wiedmann, M., and Wucherpfennig, K. W. (2002) *Cell* **111,** 967–979
35. Dadi, H. K., Simon, A. J., and Roifman, C. M. (2003) *New Eng. J. Med.* **349,** 1821–1828